SPARK PLASMA SINTERING TECHNOLOGY APPLIED TO POLYMER/METAL COMPOSITES FOR STRUCTURAL LIGHT WEIGHTING

M. Schwertz[a,b*], S. Lemonnier[a], E. Barraud[a], A. Carradò[c], M.F. Vallat[b], M. Nardin[b]

[a]*French-German Research Institute of Saint-Louis, 5, rue du Général Cassagnou, 68300 Saint-Louis, France*
[b]*Institut de Science des Matériaux de Mulhouse, UMR 7361 CNRS UHA, 15, rue Jean Starcky, 68057 Mulhouse, France*
[c]*Institut de Physique et Chimie des Matériaux de Strasbourg, UMR 7504 CNRS UDS, 23, rue du Loess, 67034 Strasbourg, France*
**e-mail address of the corresponding author: maxime.schwertz@isl.eu*

Keywords: spark plasma sintering, polymer/metal composites, joining technologies

Abstract
This paper deals with the development of polymer/metal assembly for structural applications, using the powder metallurgy (PM) route, and more precisely the spark plasma sintering (SPS) technique. In a first approach, the optimisation of polyimide (PI) consolidation by SPS was done. For temperatures as low as 320°C, relative densities higher than 99% and homogeneous mechanical properties determined by means of compression tests were achieved. In a second time, multilayered polyimide/aluminium composites were consolidated by SPS. The polymer and the polymer/metal interfaces were evaluated by a method combining compact tensile tests (CT) in order to determine the fracture toughness of each material and scanning electron microscopy (SEM) observations.

1 Introduction

Polymer/metal composite materials and more particularly sandwich material systems or functionally graded materials (FGMs) represent an interesting and effective solution for the design of advanced materials [1]. Sandwich composites, combining the low density of the polymer with the stiffness and the strength of the metal, are considered to be of great interest for high-demand engineering applications, especially in the automotive [2] and aerospace [3] industries. Their processing is conditioned by the material used for the composite development and the design of the targeted parts. In this way, various methods can be used for developing these materials and among them, the most common are the hot pressing (HP) and the roll bonding (RB) [4, 5]. In recent years, a consolidation process called - spark plasma sintering (SPS) - was pointed out as it has proven its efficiency for sintering and joining dissimilar materials in various domains and more particularly for structural as well as biomedical applications [6-11]. However, only a few studies have demonstrated the feasibility of polymer/metal composites development by this technique. Omori *et al.* [12] studied the development of FGMs prepared from aluminium (Al) and polyimide (PI) powders using a SPS apparatus. The making of such composites in one step with a consolidation temperature difference of 85°C was possible thanks to the development of a die exhibiting variable diameters generating a temperature gradient along the tool. After the consolidation, cracks

appeared in the PI and were attributed to the relaxation of residual stresses caused by the difference of thermal expansion of each material ($\alpha_{PI} = 55.10^{-6}$ °C^{-1}, while $\alpha_{Al} = 24.10^{-6}$ °C^{-1}). Therefore, the residual stresses concentrated along the PI/Al interface, caused fracture that has propagated in the PI layer as it exhibits the lowest mechanical properties. A solution to decrease these stresses was to insert composite layers with different PI/Al ratios. This solution was successfully demonstrated by the authors although the cohesion of the FGMs was only evidenced by Vickers indentation measurements along the PI/Al interface. In another work, Omori *et al.* [13] replaced Al by copper (Cu) to obtain PI/Cu FGM. A custom die was designed in order to create a temperature difference between PI and Cu. Using this die and three layers of PI and Cu powders, dense FGMs with no cracks or pores were obtained but the composite cohesion was not quantified. To conclude, only few attempts were done in the literature to study the potential of the SPS technique to develop polymer/metal assembly. To sinter both the polymer and the metal in only one step, the major problem is the difference between their consolidation temperatures, which leads in most of the case to an early degradation of the polymer. Moreover, the use of a custom die, creating a temperature gradient along the tool, may probably lead in the obtaining of heterogeneous properties of the two materials and as a result a lack of control and optimisation of the global properties.

The aim of the present work is the development of polymer/metal assembly, exhibiting high macroscopic and microscopic cohesion, and thus interesting mechanical properties for structural applications. To achieve it, the understanding of the influence of the consolidation parameters on the material properties is necessary by correlating the mechanical properties with the microstructure. Moreover, the comprehension and mechanical characterisation of the interface between the polymer and the metal is very important. The use of a thermostable PI, associated with Al, was considered as it is consistent with the mechanical and thermal properties requirements for structural parts. Firstly, the understanding of the SPS sintering condition influences on the mechanical properties of PI was studied and optimised. In a second time, the development by SPS of PI/Al assembly was envisaged through a FGM approach using intermediate layers of PI+Al with different volume ratios. The adhesion quality, and more precisely, the composite interfaces or interphases were characterised in terms of structural (SEM) and mechanical properties (CT tests) and correlated with the mechanisms involved during the consolidation of the polymer.

2 Experimental

2.1 Materials

An amorphous raw PI powder, granulated into agglomerates ranging from 400 µm to 800 µm was used. The average particle size of the primary particles was in the range between 1 µm and 10 µm. The glass transition temperature (Tg) and the theoretical density were 320°C and 1.38 g.cm^{-3}, respectively. The metallic powder used in the present study was a raw 1050 Al of 99.5% purity. The average particle size of the powder was lower than 40 µm and the theoretical density was 2.7 g.cm^{-3}.

2.2 Spark Plasma Sintering

Samples were sintered using a HP D 125 SPS facility from FCT Systeme GmbH (Rauenstein, Germany).

2.2.1 Polymer sintering

In all experiments the temperature was regulated by a K-thermocouple placed at 2 mm of the internal die surface. The powder was weighed so as to obtain 10-mm-thick pellets with a diameter of 30 mm at maximum densification. Sintering was carried out under vacuum at a heating rate of 10°C/min to ensure the temperature homogeneity inside the sample. The uniaxial pressure was gradually applied at 250°C in order to reach 40 MPa in 2 min and maintained during the following heating up to the maximum temperature, and the 5 min dwell time at the maximum temperature. The sample was then gradually cooled down to 250 °C. At this temperature, the uniaxial pressure was released in 2 min. Finally, free cooling until room temperature was applied.

2.2.2 Preparation of the polymer/metal assembly

The polymer/metal assembly was developed in 3 steps. Firstly, a 5 mm thickness Al pellet was sintered with the SPS technology at 620°C for 5 min at 50 MPa. The heating rate was fixed at 50°C/min. After sintering, no specific treatment was performed on Al surface in order to keep the roughness of the sintered material. In a second time, PI+Al blends with 75/25 and 90/10 v/v % were prepared using a three-dimensional mixer (Turbula®) during 60 min with 6 mm diameter steel balls. Then, PI+Al and PI powdery layers were successively added on the Al substrate inside the die without any compaction step. The overall PI/Al assembly was sintered following the procedure described in the *2.2.1* section.

2.3 Characterisations

2.3.1 Density measurements

The densities of the sintered samples were determined by means of helium pycnometer method (Micromeritics AccuPyc 1330).

2.3.2 Compression tests

Compression tests were carried out on PI and PI+Al specimens of 5 mm in diameter and thickness taken at three positions in the sintered pellet (Fig. 1a, C = centre; B = borderline; A = angle). The compression tests were performed with a testing machine (Instron 5500 K9400) at a crosshead displacement rate of 1 mm/min. Young's modulus (E), compressive strength (σ) and compression at break (ε) were thus determined.

2.3.3 Compact tensile (CT) tests

Compact tensile (CT) tests were performed at 10 mm/min on PI sample and PI/Al assembly following the international standard ISO 13586 [14]. Fracture toughness (G_{IC} and K_{IC}) of the materials were determined. The specimens used for these tests were cut in the diameter direction of the sintered PI pellet and in the height of the assembly. Their geometry is described in Fig. 1b.

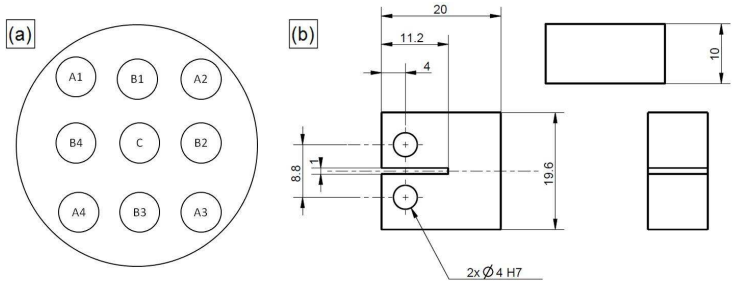

Figure 1. Sketch of (a) the different positions of the sample where the specimens were taken for the compression tests and (b) the dimensions (in mm) and geometry of the specimens used for the CT tests.

K_{IC} was calculated from the load F at crack growth initiation (given by the load-displacement curve of the CT tests) and the original crack length a ($7.2.10^{-3}$ m) given by Eq. 1 [14]:

$$K_{IC} = f(a/w) \cdot \frac{F}{h \cdot \sqrt{w}} \tag{1}$$

where h is the test specimen thickness (10.10^{-3} m); w is the test specimen width (16.10^{-3} m); $f(a/w)$ is the geometry calibration factor calculated according to Eq. 2 [14]:

$$f(a/w) = f(x) = \frac{(2+x)}{(1-x)^{3/2}} \cdot (0.886 + 4.64x - 13.32x^2 + 14.72x^3 - 5.6x^4) \tag{2}$$

with $x = 0.45$ and $f(0.45) = 8.34$ .Then, G_{IC} was obtained according to Eq. 3 [14]:

$$G_{IC} = (1-\nu^2) \cdot \frac{{K_{IC}}^2}{E_{fract}} \tag{3}$$

where ν is the Poisson's ratio (0.41 corresponding to the PI value as it corresponds to the polymer matrix) and E_{fract} the elasticity modulus obtained at the same time and temperature conditions as the fracture test, corresponding to the linear slope from the test beginning to the crack growth initiation

2.3.4 Scanning electron microscopy (SEM)

After the mechanical tests, the fracture surfaces of the specimens and the polymer/metal interfaces were observed by scanning electron microscopy (SEM, FEI Nova NanoSEM 450).

3 Results and discussion

3.1 PI consolidation by SPS technology

PI samples were sintered at two different temperatures: 300°C and 320°C. Relative densities higher than 99% were achieved in both cases. In order to evaluate the influence of sintering temperature on the material properties and more particularly on the homogeneity of the

sample, density measurements were combined with compression tests. The compression curves reported in Fig. 2 show the influence of the dwell temperature on the bulk properties but also on their homogeneity throughout the PI sample.

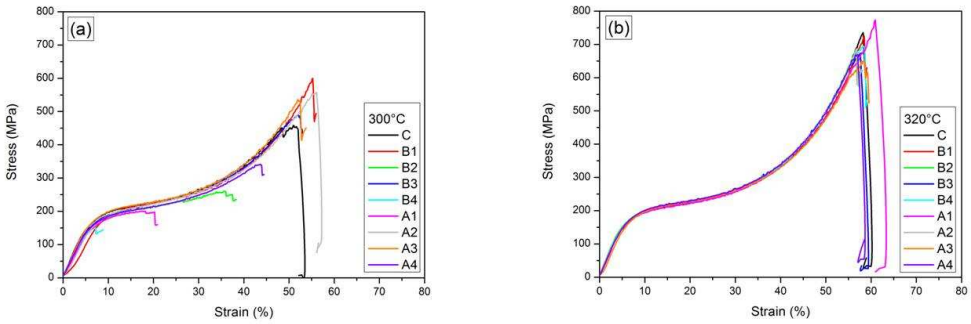

Figure 2. Compression curves of specimens taken in the pellets sintered at (a) 300°C and (b) 320°C according to the positions defined in Fig. 1a.

At 300°C (Fig. 2a), only the B4 specimen breaks in the elastic zone. The failure of the other specimens is observed either in the plastic zone (A1, B2 and A4) or in the viscoplastic one (C, B1, B3, A2 and A3). For this sintering temperature, homogeneous mechanical properties have not been obtained in the sintered pellet. By contrast, at 320°C (Fig. 2b), the compression curves are very reproducible. All the specimens break in the viscoplastic zone, at a compressive stress of about 700 MPa, corresponding to a compression ratio of approximately 60%, which are the highest values reported in the literature, to our knowledge, for an unfilled sintered thermoplastic PI [15, 16]. At 320°C, the mobility of polymer chains is higher than at 300°C as the temperature is very close to Tg. It leads to a better inter-diffusion of the macromolecular chains at the interface of the particles and results in a better cohesion between the particles and the obtaining of homogeneous mechanical properties.

3.2 PI/PI+Al/Al assembly development by SPS technology

Once the polymer consolidation parameters were set up in order to get homogeneous mechanical properties, the development of PI/PI+Al/Al FGMs was studied. In a first approach, assemblies were envisaged without any interlayer between the raw PI and the raw Al. The PI powder was poured on the Al pre-sintered layer inside the die and the whole was consolidated following the optimised cycle for the PI sintering. Low cohesion at the interface was observed as shown on the SEM image in Fig. 3. It was not possible to carry out the mechanical characterisation of the interface as it broke when cutting the sample. This rupture can be attributed to the thermal expansion difference between the PI and the Al as their coefficients are 55.10^{-6} °C^{-1} and 24.10^{-6} °C^{-1}, respectively.

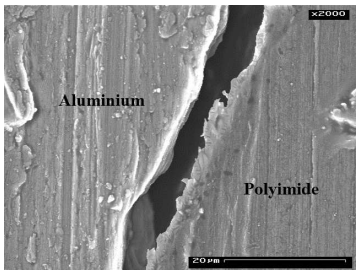

Figure 3. SEM image of PI/Al assembly interface.

To improve the interfacial strength between PI and Al, the addition of an interlayer was studied. This interlayer was composed of a blend of PI+Al. In this way, it is expected that this layer exhibits intermediate thermal expansion coefficient leading to softer transition between the layers. Two compositions of interlayer were studied, 90/10 and 75/25 PI+Al v/v %. PI/PI+Al/Al assembly was developed following the optimised sintering cycle of the PI. The mechanical characterisations of the two compositions of interlayers were carried out by means of compression test and the results are summarised in Table 1.

PI+Al v/v %	Density (g.cm^{-3})	E (GPa)	$\varepsilon_{(max)}$ (%)	$\sigma_{(max)}$ (MPa)
100/0	1.38 ± 0.01	3.3 ± 0.1	60 ± 1	707 ± 27
90/10	1.50 ± 0.01	3.5 ± 0.1	59 ± 1	715 ± 23
75/25	1.70 ± 0.01	4.1 ± 0.1	56 ± 1	596 ± 25

Table 1. Densities and mechanical properties of PI and PI+Al interlayers.

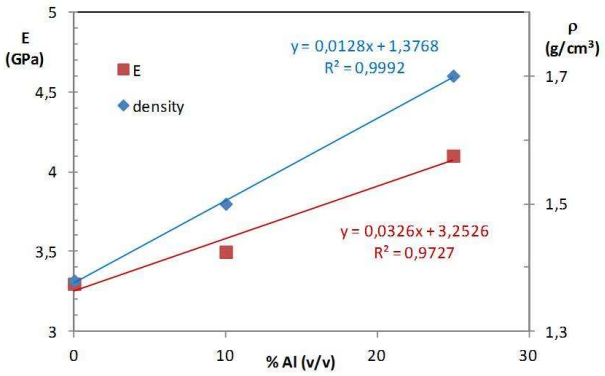

Figure 4. Young's modulus and density of PI+Al interlayers as function of the volume fraction of Al powder.

Fig. 4 shows a good correlation between Young's modulus and density with the volume fraction of Al powder. An increase in the volume percentage of Al in the interlayer leads to a linear increase of the density, as well as of *E* compared with the unfilled PI, following a rule of mixtures. On the contrary, both ε and σ decrease when the volume fraction of Al increases. Finally, the unfilled PI and the PI+Al 90/10 v/v % interlayer composite display almost the same compressive strength and compression at break. In the following, the PI+Al 75/25 v/v % composite was chosen as interlayer for the development of PI/PI+Al/Al FGMs because its larger ratio of Al leads to a better compromise between thermal expansions of Al and PI and as a result a decrease of the residual stresses at the interfaces. Moreover, its rigidity is enhanced compared with the unfilled PI while its ductility is only slightly reduced. Thus, PI/PI+Al/Al FGMs were successfully made as illustrated by the cross section image in Fig. 5. SEM observations of PI/PI+Al and PI+Al/Al interfaces are shown in Fig. 6a and 6b.

Figure 5. Image of PI/PI+Al/Al FGM cross section obtained by SPS.

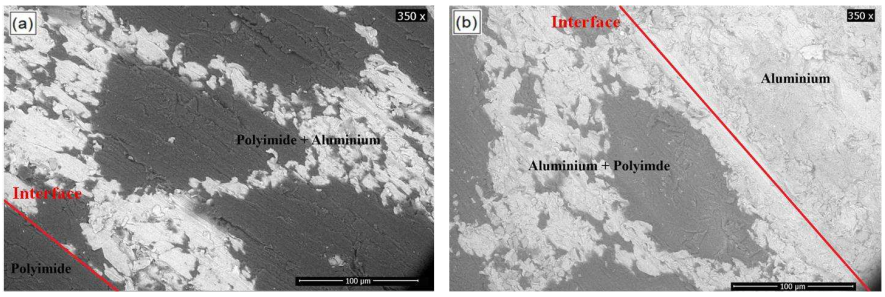

Figure 6. SEM images of (a) PI/PI+Al and (b) PI+Al/Al interfaces represented by the red line.

As illustrated in Fig. 6, the PI/PI+Al and PI+Al/Al interfaces are not discontinuous as in Fig. 3. The PI+Al interlayer composite has created an interphase between the unfilled PI and the sintered Al. According to macroscopic and microscopic observations, a strong cohesion of the assembly is assumed. To confirm these observations, CT tests were performed in order to determine the K_{IC} and G_{IC} values. Firstly, CT tests were realised on unfilled PI to compare the fracture toughness of the PI with the one of the assembly. The values obtained are K_{IC} of 1.66 MPa.m$^{1/2}$ and G_{IC} of 0.79 kJ.m^{-2}. These PI values are in agreement with values reported in the literature [17-19] and in the same order of magnitude as rigid structural polymers such as polyester resin and epoxy resin [20]. Then, the characterisation of PI/PI+Al and PI+Al/Al interfaces was envisaged. However, only PI/PI+Al interfaces were addressed because the PI+Al/Al interfaces broke, due to the introduction of stresses and solicitations, at the interface during the cut of the complex geometry of the CT test specimen. Improvements of PI+Al/Al interfaces are currently under study notably thanks to a surface treatment of the raw Al surface, leading to a better cohesion between Al and PI+Al layers. The PI/PI+Al specimen is shown in Fig. 7a. For failure loads of 480 N and 325 N, K_{IC} are equal to 3.16 MPa.m$^{1/2}$ and 2.14 MPa.m$^{1/2}$, respectively. The two values display an important difference whereas the measures correspond to two specimens taken in the same sintered sample. This discrepancy can be attributed to an inhomogeneous blend of the PI+Al powders leading to a different behaviour and propagation of the crack at the interface. For both tests, the fracture occurred in the unfilled PI layer meaning that the PI/PI+Al interface created is stronger than the PI one. Finally, for loads of 325 N and 480 N, and thanks to the E_{fract} values given by Fig. 7b, G_{IC} calculated are 3.47 kJ.m^{-2} and 7.14 kJ.m^{-2}, respectively. All the CT test results are summarised in Table 2.

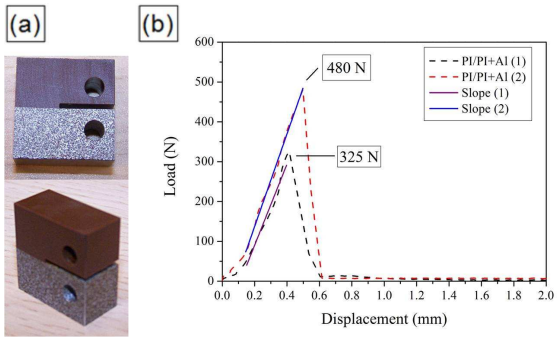

Figure 7. (a) Images and (b) load-displacement curves of PI/PI+Al CT specimens.

Finally, the fracture toughness of the PI/PI+Al composite is higher than the PI one, confirming that the interface created is stronger that the polymer. However, complementary CT tests are currently in progress to enhance the reproducibility and the standard error on such a test.

Load (N)	*Slope*	E_{fract} *(MPa)*	K_{IC} *(MPa.m$^{1/2}$)*	G_{IC} *(kJ.m^{-2})*
325	(1)	1019 ± 41	2.14	3.47
480	(2)	1163 ± 14	3.16	7.14

Table 2. *CT test* results of PI/PI+Al composites.

Conclusions

In order to obtain PI/Al FGMs, the aim of this work is to study the PI consolidation and the PI/Al assembly by the SPS technology. The results of the PI mechanical properties shows that the homogeneity inside the sample is achieved by increasing the sintering temperature so that it is equal to or above to the glass transition temperature (Tg) of the PI. The compressive strength of PI approximately reaches about 700 MPa at a compression strain of 60%, which are the highest values, to our knowledge, reported in the literature for an unfilled and sintered PI. In a first approach, cohesive PI samples and PI/PI+Al/Al FGMs were obtained by means of the SPS method at 320°C for a sintering cycle of less than one hour. The development of such assembly was obtainable thanks to the addition of a PI+Al interlayer composed of PI+Al 75/25 v/v %. The different interfaces were characterised by SEM observations and CT tests to determine the fracture toughness. The PI/PI+Al composites displayed K_{IC} and G_{IC} values of 2.14 and 3.16 MPa.m$^{1/2}$ and 3.47 and 7.14 kJ.m^{-2}. Improvements of PI+Al/Al interfaces are currently under study in order to obtain a better cohesion between Al and PI+Al layers.

References

[1] B. Harris. A perspective view of composite materials development. *Materials & Design*, 12 (5): 259-272, 1991.
[2] D. Mohr, G. Straza. Development of formable all-metal sandwich sheets for automotive applications. *Advanced Engineering Materials*, 7 (4): 243-246, 2005.
[3] N. W. Bailey, M. A. Battley, M. Zhou. Experimental method for dynamic residual strength characterisation of aircraft sandwich structures. *International Journal of Crashworthiness*, 18 (1): 64-81, 2013.
[4] O. A. Sokolova, A. Carradò, H. Palkowski. Metal–polymer–metal sandwiches with local metal reinforcements: A study on formability by deep drawing and bending. *Composite Structures*, 94 (1): 1-7, 2011.
[5] A. Carradò, J. Faerber, S. Niemeyer, G. Ziegmann, H. Palkowski. Metal/polymer/metal hybrid systems: Towards potential formability applications. *Composite Structures*, 93 (2): 715-721, 2011.
[6] M. Tokita, Ieee. *Industrial applications for functionally graded materials fabricated by spark plasma sintering (SPS) systems*. Ieee, New York, 2000.
[7] Z. J. Shen, M. Johnsson, M. Nygren. TiN/Al2O3 composites and graded laminates thereof consolidated by spark plasma sintering. *Journal of the European Ceramic Society*, 23 (7): 1061-1068, 2003.
[8] Y. Makino, K. Mizuuchi, M. Tokita, Y. Agari, M. Kawahara, K. Inoue. Synthesis of new structural and functional materials by SPS processing In T. Chandra, N. Wanderka, W. Reimers, M. Ionescu, *Thermec 2009, Pts 1-4*, 2091-2096. Trans Tech Publications Ltd, Stafa-Zurich, 2010.
[9] M. Tokita. The potential of Spark Plasma Sintering (SPS) method for the fabrication on an industrial scale of Functionally Graded Materials. *Advances in Science and Technology*, 63: 322-331, 2010.
[10] Y. Watanabe, Y. Iwasa, H. Sato, A. Teramoto, K. Abe. Fabrication of Titanium Biodegradable-polymer FGM for Medical Application. In A. Kawasaki, A. Kumakawa, M. Niino, *Multiscale, Multifunctional and Functionally Graded Materials*, 199-204. 2010.
[11] Y. Watanabe, Y. Iwasa, H. Sato, A. Teramoto, K. Abe, E. Miura-Fujiwara. Microstructures and mechanical properties of titanium/biodegradable-polymer FGM for bone tissue fabricated by spark plasma sintering method. *Journal of Materials Processing Technology*, 211 (12): 1919-1926, 2011.
[12] M. Omori. *Functionally Gradient Materials from Al and Polyimide of the paper*. In 3rd International Symposium on Structural and Functional Gradient Materials, 667-671, 1994.
[13] M. Omori, A. Okubo, G. H. Kang, T. Hirai. Preparation and properties of polyimide/Cu functionally graded material. In S. Ichiro, M. Yoshinari, *Functionally Graded Materials 1996*, 767-772. Elsevier Science B.V., Amsterdam, 1997.
[14] ISO 13586:2000(E). *Plastics — Determination of fracture toughness (G_{IC} and K_{IC}) — Linear elastic fracture mechanics (LEFM) approach*, 2000.
[15] D.-J. Liaw, K.-L. Wang, Y.-C. Huang, K.-R. Lee, J.-Y. Lai, C.-S. Ha. Advanced polyimide materials: Syntheses, physical properties and applications. *Progress in Polymer Science*, 37 (7): 907-974, 2012.
[16] C. E. Sroog. Polyimides. *Progress in Polymer Science*, 16 (4): 561-694, 1991.
[17] F. W. Harris, H.-S. Lien, P. A. Gabori, Y. Zhang, T. M. Chalmers, A. Zhang, D. Shen, S. Z. D. Cheng. A new semicrystalline, thermoplastic polyimide for carbon fiber-reinforced composites. *Composite Structures*, 27 (1–2): 17-23, 1994.
[18] J. A. Hinkley, S. L. Mings. Fracture toughness of polyimide films. *Polymer*, 31 (1): 75-77, 1990.
[19] T. Bullions, R. H. Mehta, B. Tan, J. E. McGrath, D. Kranbuehl, A. C. Loos. Mode I and Mode II fracture toughness of high-performance 3000g.mole−1 reactive poly(etherimide)/carbon fiber composites. *Composites Part A: Applied Science and Manufacturing*, 30 (2): 153-162, 1999.
[20] H. Kausch. Chapter 9: Molecular Chains in Heterogeneous Fracture. In *Polymer Fracture 2 - Polymers: Properties and applications*, 260-266. Springer Berlin-Heidelberg, New-York, 1978.